



Hardness prediction of a cold rolled Nimonic 80A exhaust valve spindle

S.W. Kang ^a, S.J. Heo ^b, J.H. Yoo ^b, J.H. Kang ^{c,*}

^a Friend Co. LTD, 9, Gwahaksandan-ro 333beon-gil, Busan, 46749, Korea

^b Graduate School, Department of Convergence Engineering, Jungwon Univ., 85, Munmuro, Chungbuk, 28024, Korea

^c Department of Aero-Mechanical Engineering, Jungwon Univ., 85, Munmuro, Chungbuk, 28024, Korea

* Corresponding e-mail address: jhkang@jwu.ac.kr

ABSTRACT

Purpose: of this paper is to predict the hardness of cold rolled exhausts valve spindle fabricated of Nimonic 80A via axisymmetric finite element analysis, compression testing, and hardness inspection.

Design/methodology/approach: The stress-strain relationship of Nimonic 80A was obtained via compression testing with deformation ratios of 10%, 20%, and 30%. Hardness changes caused by the strain hardening effect were measured in cut specimens in both the axial and circumferential directions following compression testing. The effective strain at the measurement position was calculated via finite element analysis. The regression equation for hardness changes caused by work hardening was derived from analysed strain and inspected hardness. The cold-rolling deformation of an exhaust valve spindle was analysed using axisymmetric finite element analysis.

Findings: The stress-strain relationship calculated from compression testing was well expressed using the Holloman equation and the strain-hardness relationship by strain hardening was successfully regressed using the shifted power law model for Nimonic 80A, Nickel-Chromium based super alloy.

Research limitations/implications: This research focused hardness prediction of spindle after ring rolling operation for generating beneficial compressive surface residual stresses for enhancing fatigue life. Further research to quantify compressive residual stress after rolling shall be followed to increase fatigue life.

Practical implications: The cold rolling process is a typical incremental forming method and should be analysed under three-dimensional conditions. However, it takes lots of time to solve incremental forming analysis. To predict hardness distribution after rolling in the manufacturing field, FE analysis was performed under two-dimensional axisymmetric conditions based on the assumption of no friction generated by the rolling tool. The deformed shapes and hardness distribution from the inspection quality standard and two-dimensional FE analysis showed very similar results. Simplified finite element analysis method for ring rolling process for local area could be very effective method in the industrial field.

Originality/value: The stress-strain relationship and the hardness and strain relationship were derived by compression test and hardness measurement for compressed specimen for Nimonic 80A, Nickel-Chromium based super alloy. And simplified finite element analysis method was suggested to predict deformed shape and hardness distribution of locally cold

rolled region and achieved similar result between FE analysis result and Quality standard. Suggested method would be very effective method to engine spindle manufacture to predict hardness of different size of product.

Keywords: Nimonic 80A, Exhaust valve, Stress-strain curve, Hardness prediction, Finite element method

Reference to this paper should be given in the following way:

S.W. Kang, S.J. Heo, J.H. Yoo, J.H. Kang, Hardness prediction of a cold rolled Nimonic 80A exhaust valve spindle, Journal of Achievements in Materials and Manufacturing Engineering 94/1-2 (2019) 13-21.

ANALYSIS AND MODELLING

1. Introduction

The exhaust valve spindle is an important component of marine diesel engines. It is located at the top of the engine cylinder and controls the release of high-temperature and high-pressure gas following the combustion process of the engine cycle. Therefore, it must withstand high-temperature conditions according to different operating conditions and provide mechanical durability to withstand repeated combustion events [1-4].

The exhaust valve spindle in a marine diesel engine is constantly affected by exhaust gases at high temperatures (Fig. 1). Therefore, superalloys, such as Nimonic and Inconel, are used to prevent the degradation of strength at high temperatures. In particular, the contact area between the exhaust valve spindle and valve seat requires excellent fatigue characteristics based on the presence of high impact stress combined with high service temperatures in a corrosive environment. Current exhaust valve spindles are typically fabricated from Nimonic 80A or Duraspindle which is welded with an Inconel to austenitic stainless steel base metal at seat valve contact area [5-6].

This study focused on a work hardening process to improve the fatigue characteristics of exhaust valve spindle fabricated from Nimonic 80A. This process should reduce or eliminate residual tensile stresses generated during manufacturing, heat treating, and welding to improve the fatigue life of steel materials. A greater tensile strength for given steel results in a greater fatigue limit [7]. Generally, compressive residual stress at the surface also increase the fatigue limit. The most widely used mechanical processes for generating beneficial compressive surface residual stresses for enhancing long and intermediate fatigue life are shot-peening and surface rolling [8]. We conducted a quantitative study to investigate the effects of cold rolling on marine engine parts in terms of residual stress and fatigue life [9]. Past studies have also shown that compressive stress increases the fatigue life of both cast steel and wrought steel [10].

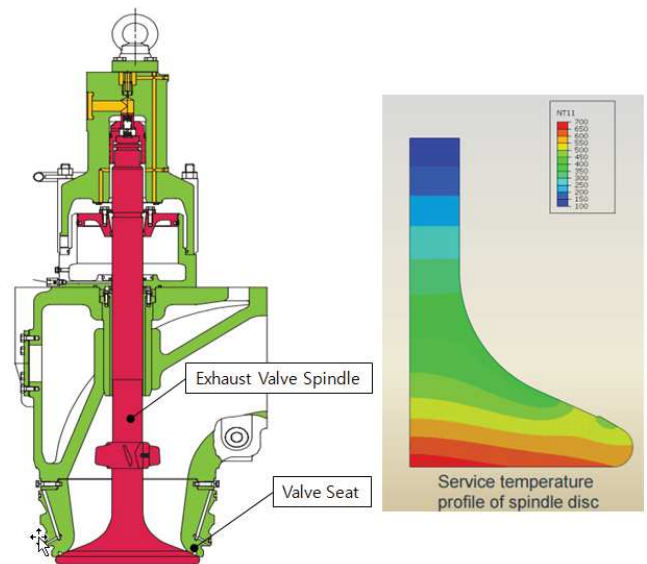


Fig. 1. Exhaust valve structure and temperature distribution of valve spindle [5-6]

Residual stress on the surface of steel is introduced by the cold rolling method. To ensure the generation of compressive residual stress, a certain level of plastic deformation must be applied. It is possible to determine if residual stress has been generated by measuring the hardness of the plastic deformation region to guarantee a certain amount of plastic deformation. A study on the relationship between plastic deformation and hardness was carried out to quantify the relationship between hardness and true strain in the backward extrusion process. Excellent coincidence between measured hardness and hardness predicted using finite element (FE) analysis was demonstrated [11-12]. Additionally, a relationship between strain and hardness was formulated using the definition of Brinell hardness and calculated hardness by formulation was validated through comparisons to experimentally inspected hardness [13].

In this study, Nimonic 80A was subjected to compression tests with deformation ratios of 10%, 20%, and 30% and hardness was measured in both the axial and circumferential directions. The effective strain at the hardness measurement position was calculated by performing simple upsetting analysis using the Deform 2D Commercial Software. This allowed us to derive a relationship between effective strain and hardness. FE analysis was performed on the cold rolling process using the flow stress obtained from compression testing. The validity of hardness prediction using two-dimensional FE analysis was verified by comparing the deformed shape and predicted hardness to the shape and hardness required by cold rolling specifications.

2. Experiment

2.1. Compression testing

An exhaust valve spindle hot forged from Nimonic 80A was subjected to cold rolling following heat treatment and rough machining. Localized large deformation occurs at room temperature during the cold rolling process, meaning a stress-strain relationship is required for deformation analysis. The stress-strain relationship was obtained via compression testing. Table 1 lists the alloying elements of the Nimonic 80A material used for the compression specimen

Table 1.
Chemical composition of Nimonic 80A (wt.%)

Chemical	Range	Mill Sheet
Carbon	0.10 max.	0.042
Manganese	1.0 max.	0.04
Phosphorus	0.015 max.	0.004
Sulfur	0.015 max.	0.004
Silicon	1.0 max.	0.06
Chromium	18.0~21.0	19.87
Nickel	Balance	74.85
Copper	0.2 max.	0.01
Titanium	1.8~2.7	2.57
Aluminium	1.0~1.8	1.65
Iron	3.0 max	0.84
Cobalt	2.0 max	0.06
Boron	0.008 max	0.004
Zirconium	0.15 max	0.01

Compression specimens were machined to dimensions of $\Phi 10 \times 12$ mm. The specimens were compressed by 10%, 20%, and 30% of their height to determine the forming load. The compression testing was carried out at a strain rate of 0.01 mm/mm/sec and a liquid lubricant was introduced to reduce the frictional force. Figure 2 presents the stress-strain curve calculated from the displacement and load during compression testing. The stress-strain curve calculated from compression testing was regressed using the Holloman equation and is expressed by Eq. (1):

$$\sigma = 1739.5 \varepsilon^{0.1058}, \text{ MPa} \quad (1)$$

where: σ – flow stress, ε – effective strain.

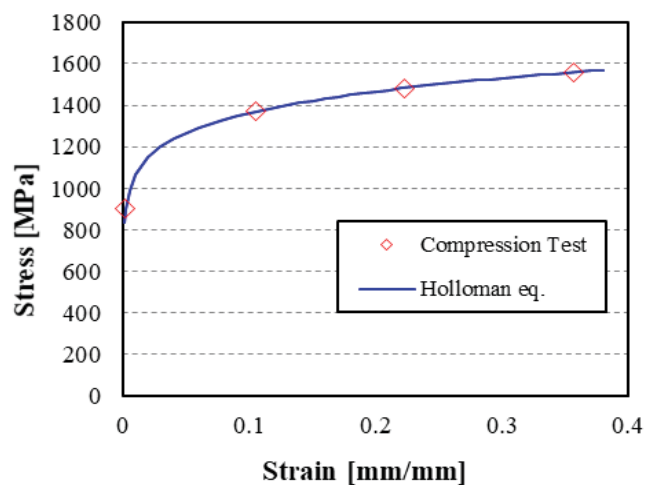


Fig. 2. Stress-strain derived by compression testing

2.2. Hardness inspection

The hardness testing specimens were manufactured by cutting the 10%, 20%, and 30% compressed cylinders in the axial and circumferential directions. Axial-direction hardness was measured at the centre and end of the cut surface perpendicular to the axial direction. Circumferential-direction hardness was measured at nine different points because strain varied depending on the position of the specimen. The hardness measurement positions and directions are illustrated in Figure 3.

The strain distribution varies based on the positions of the specimens obtained from compression testing. Simple upset FE analysis was performed to analyse the positional strain of the samples. FE analyses were performed using the Deform 2D Commercial Software and the flow stress obtained from compression testing was applied. The friction between the material and dies was

modelled with a value of 0.05, which is the friction coefficient of the liquid lubricant. Figure 4 presents the deformation shape and strain distributions of the 10%, 20%, and 30% upset samples.

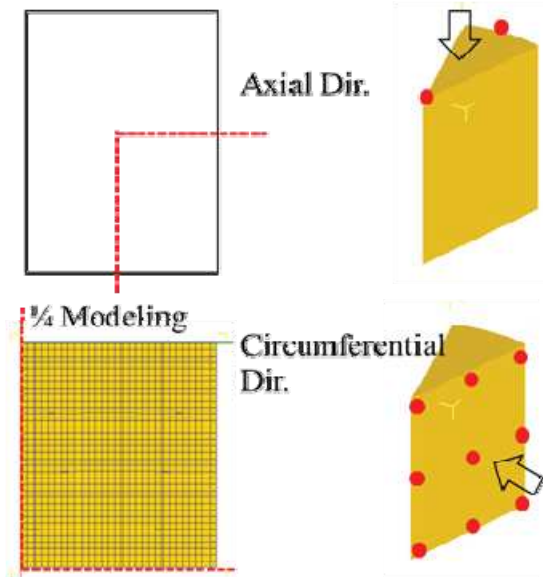


Fig. 3. Hardness measurement directions and positions

Figure 5 presents the cutting plan for the upset samples for preparing hardness specimens, as well as the axial-direction hardness measurement position. Axial-direction specimens were prepared by the cutting the upset samples horizontally. One point at the centre of the axial specimen and eight points at the distal end of the outer diameter were measured perpendicular to the plane of the cut. Circumferential-direction specimens were cut horizontally from the upset samples, then cut in the vertical direction. For the convenience of hardness measurement, specimens were prepared with plastic mounting, as shown in Figure 5(b). Hardness was measured in both axial and circumferential directions. The measured results are summarized in Table 2.

The axial-direction hardness and circumferential-direction hardness are plotted in Figure 6. The hardness values corresponding to the flow stresses for the 10%, 20%, and 30% compression specimens, as well as the 0.2% offset strength of Nimonic 80A, are also included in Figure 6. The strain-hardness relationship at all points shown in Figure 6 was regressed using the shifted power law model and is expressed by Eq. (2):

$$HV = 548.5(\epsilon+0.0108)^{0.1363} \quad (2)$$

where: HV – Vickers hardness, ϵ – effective strain.

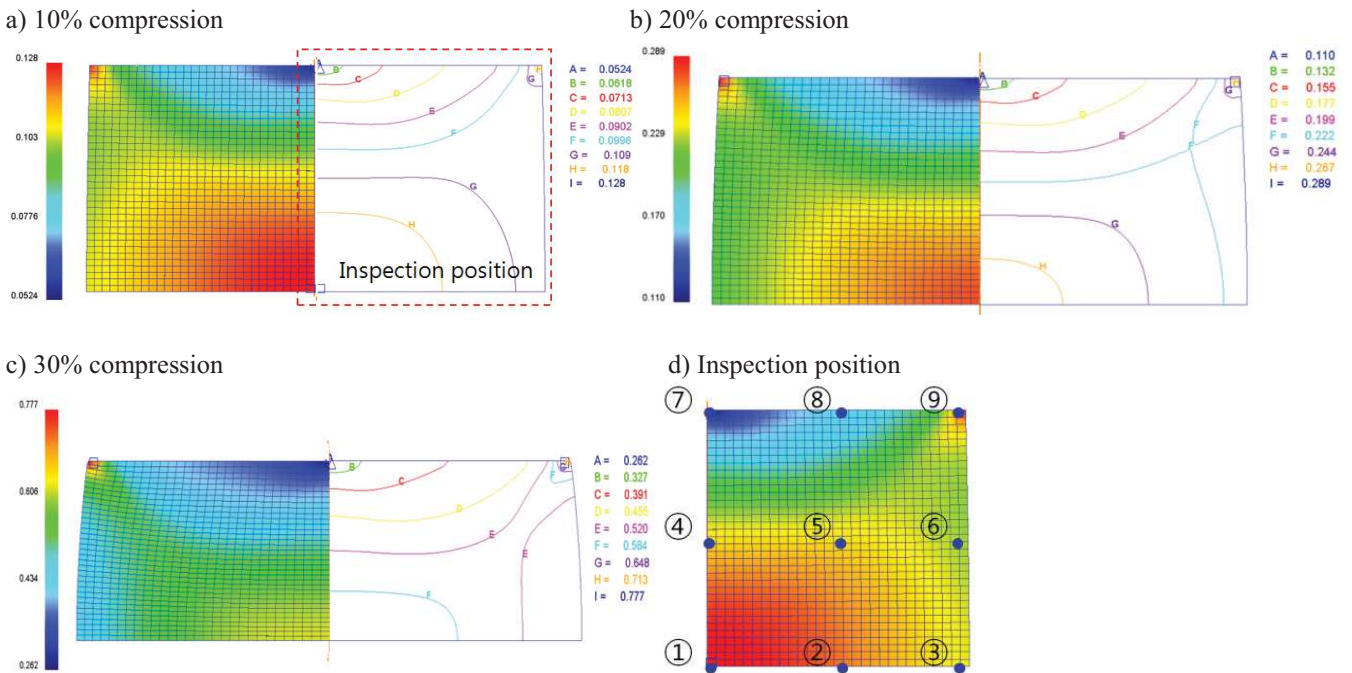
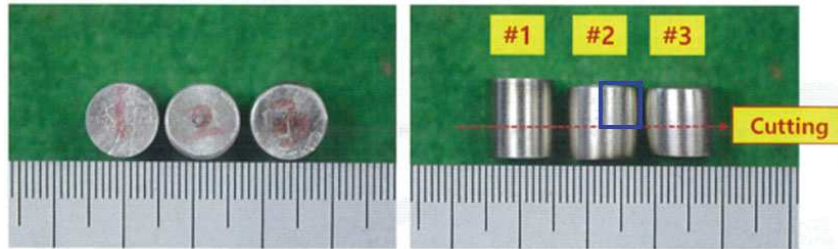


Fig. 4. True strain distributions according to the position of a compression specimen

a) Cutting plan for compression testing specimens



b) Hardness specimen preparation and inspection locations



Fig. 5. Hardness inspection specimens

Table 2.

Hardness inspection results sorted by inspection direction and deformation ratio

Direction	Position	10%		20%		30%	
		Strain	Hardness, HV	Strain	Hardness, HV	Strain	Hardness, HV
Axial	a	0.05	412	0.11	466	0.336	477
	b	0.05	412	0.11	459	0.336	485
	c	0.05	386	0.11	473	0.336	479
	d	0.05	418	0.11	438	0.336	477
	e	0.128	455	0.276	484	0.443	518
	f	0.05	397	0.11	475	0.336	477
	g	0.05	407	0.11	455	0.336	485
	h	0.05	388	0.11	460	0.336	479
	i	0.05	400	0.11	460	0.336	477
Circumferential	1	0.128	400	0.276	478	0.443	490
	2	0.109	389	0.229	456	0.36	462
	3	0.0524	382	0.11	433	0.176	440
	4	0.12	429	0.255	455	0.409	476
	5	0.109	404	0.231	435	0.363	464
	6	0.0778	390	0.166	452	0.269	465
	7	0.106	403	0.218	437	0.34	466
	8	0.102	398	0.215	440	0.34	459
	9	0.116	402	0.279	446	0.445	465

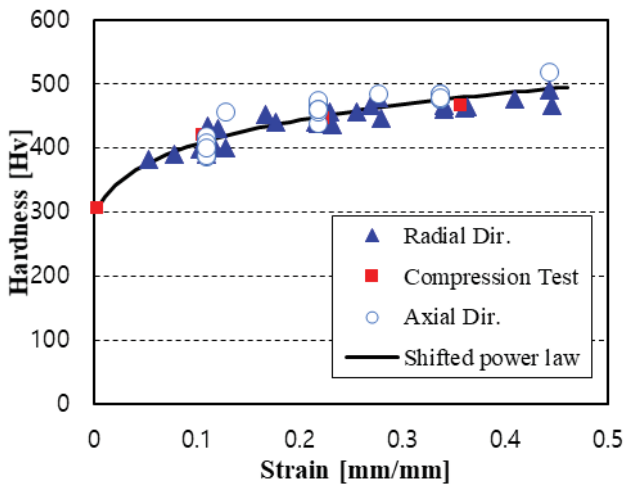


Fig. 6. Comparison of hardness inspection and interpolation results

The measured hardness in the axial direction is greater than the values predicted by the regression formula, whereas the measured hardness in the circumferential

direction is slightly lower than the values predicted by the regression formula. This may be a result of positional error of vertical cuts during circumferential specimen preparation.

3. Rolling analysis

The cold rolling process is only performed locally in the contact area with the valve seat following hot forming and rough machining. The entire process, including the rolling process, is presented in Figure 7. The rolling process forms three or four rows based on the width of the valve seat. The rolling operation time per row is 30 to 35 s and the operating pressure is 10 kgf/cm². The rolling depth is 2.1 mm and the spindle rotation speed is 150 RPM.

The cold rolling operation is a process that increases hardness in the contact area with the valve seat. There is no rotational force on the rolling tool and only compressive force along the rolling direction is applied. If friction is ignored, the cold rolling process is believed to mimic the deformation to the two-dimensional axisymmetric problem.

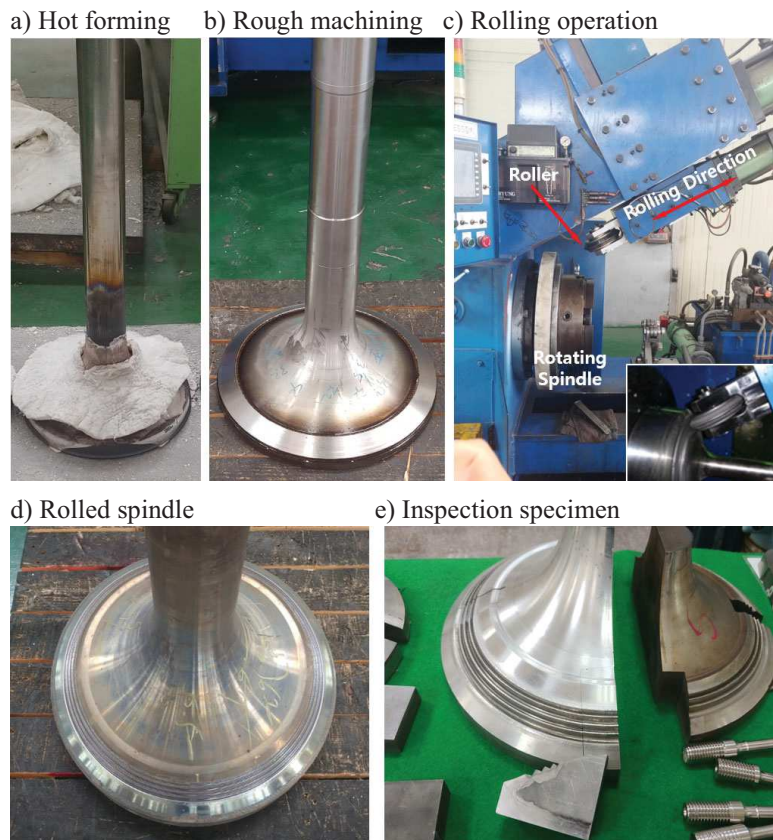


Fig. 7. Spindle preparation and cold rolling operation

The rolling process, which is a typical incremental forming method, requires very long analysis time because local deformation in small areas compared to the total size of a product requires high mesh density. In this study, two-dimensional axisymmetric analysis was conducted to reduce analysis time and increase analysis precision in local regions.

The rolling tool is assumed to be a rigid body and the motion of the tool in the rolling direction is controlled by a forming velocity of 1 mm/sec. The friction coefficient between the mould and material was assumed to be 0.05. The clamping jig is considered to be a rigid body die with no movement. The Holloman equation shown in Eq. (1) is applied as the flow stress of deformation body. In this study, a three-row rolling operation was conducted based on the small width of the valve seat. Cold rolling was performed continuously from the inside to the outside, as shown in Figure 8. Because only local deformation appears during each rolling operation, the magnified rolled shapes of each process are presented in Figures 8 (b), (c), and (d).

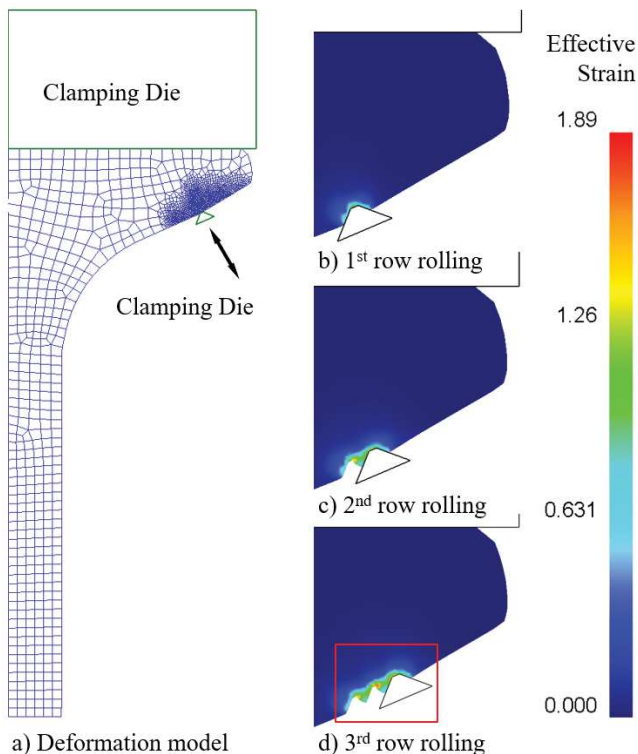


Fig. 8. FE analysis model for cold rolling and analysis results

To verify the consistency of the results of FE analysis under two-dimensional axisymmetric conditions, defor-

mation shape and hardness prediction results based on strain were compared with to the quality inspection standards for cold rolling products. The magnified shape of the rolled section is presented in Figure 9(a) and the rolled shape of the four-row product in the standard is presented in Figure 9(b). One can see that the shape of the rolling profile from our analysis is very similar to that from the standard. By substituting the effective strain value obtained from the results of forming analysis into Eq. (2), it is possible to predict the hardness increase caused by strain hardening. The strain and hardness distributions generated by cold rolling are presented in Figure 9(a). Figure 9(b) presents the required hardness distribution of a cold rolled spindle based on the quality standard [14]. Figures 9(a) and 9(b) display very similar hardness distributions.

4. Conclusions

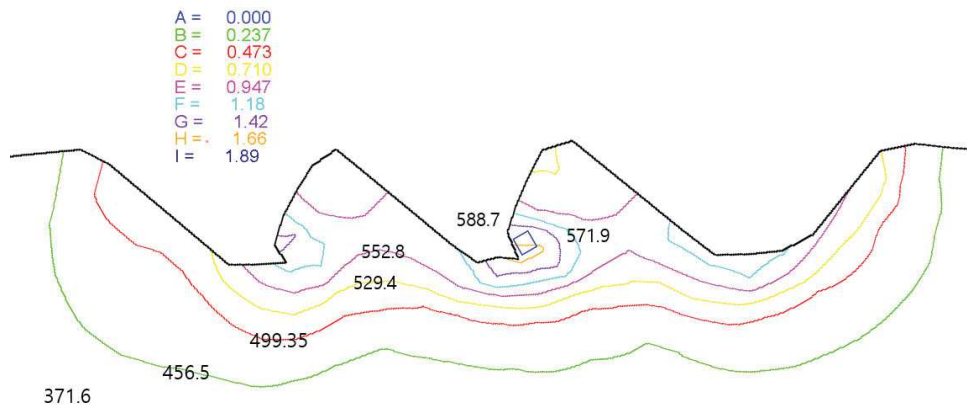
The following results were obtained from our study on predicting the hardness increase of an exhaust valve spindle fabricated of Nimonic 80A for a marine diesel engine caused by the cold rolling process.

- 1) Nimonic 80A was compressed at room temperature by ratios of 10%, 20%, and 30%, and stress and strain data were calculated from the experimental results. The stress-strain relationship of Nimonic 80A exhibits strain hardening curves similar to those of a typical ferrous metal.
- 2) The hardness of the compressed specimens was measured in both the axial and circumferential directions, and upset FE analysis was performed based on the flow stress results obtained from our experiments. The correlation between the strain and hardness of the test specimens was found to be in good agreement with the work hardening formula as demonstrated by the tensile test. The hardness prediction formula was expressed as a shifted power law model in this paper.
- 3) The cold rolling process is a typical incremental forming method and should be analysed under three-dimensional conditions. However, FE analysis was performed under two-dimensional axisymmetric conditions based on the assumption of no friction generated by the rolling tool. The deformed shapes from the inspection quality standard and two-dimensional FE analysis were compared and found to be virtually identical.

4) Validation of hardness prediction using two-dimensional FE analysis of the rolling process was performed by verifying that the predicted hardness

distributions were in good agreement with the requirements of the quality standard for Nimonic 80A valve spindles.

a) Strain and hardness distribution at rolled groove based on FE analysis



b) Hardness distribution of an exhaust valve based on the inspection standard [14]

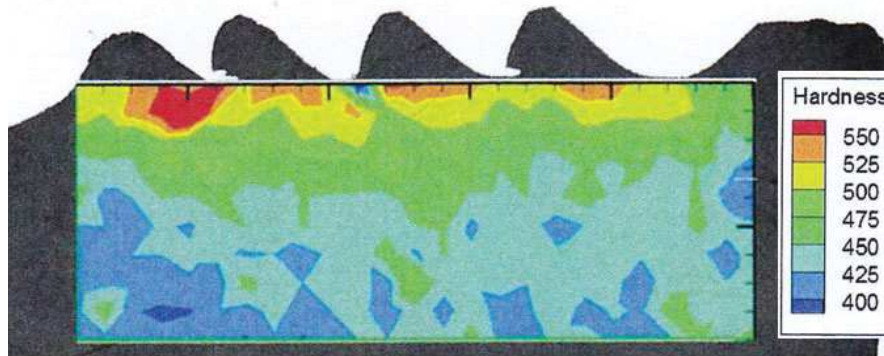


Fig. 9. Comparison of hardness analysis and inspection standard distributions

Acknowledgements

This work was supported by the Technology Innovation Program (No.: 10067300, "Development of forming technology for high corrosion resistant and heat-resistant fasteners with a hard forming material") funded By the Ministry of Trade, industry & Energy (MI, Korea).

References

- [1] U.D. Bihlet, H.A. Hoeg, Future HFO/GI exhaust valve spindle, Proceedings of the 27th CIMAC World Congress on Combustion Engine Technology, Shanghai, China, 2013.
- [2] J.V. Carstensen, Wear loaded components in large ship diesel engines, MAN Diesel & Turbo, 2012.
- [3] MAN B&W S50ME-B9.5-TII Project Guide Electronically Controlled Two stroke Engines with Camshaft Controlled Exhaust Valves, MAN Diesel & Turbo, 2016.
- [4] H. Fellmann, T. Groß, T. Ludwig, Typical wear mechanism of 2-stroke exhaust valves, Proceedings of the Marine Propulsion Conference, 2004.
- [5] N. Vardar, A. Ekerim, Investigation of Exhaust Valve Failure in Heavy-duty Diesel Engine, Gazi University Journal of Science 23/4 (2010) 493-499.

- [6] S.H. Jang, J.H. Choi, Study on reconditioning the exhaust valve of a two-stroke diesel engine, *Journal of the Korean Society of Marine Engineering* 41/6 (2017) 489-494, DOI: <https://doi.org/10.5916/jkosme.41.6.489>.
- [7] L.J. Ebert, Fatigue Resistance of Steels, in: Volume 1: Properties and Selection: Irons, Steels, and High-Performance Alloys, ASM Handbook, 1990, 673-688.
- [8] A. Fatemi, Chapter 8 – Residual Stresses & Their Effects, University of Toledo, Available at: https://www.efatigue.com/training/Chapter_8.pdf.
- [9] M. Matsuda, E. Ootsuki, S. Kajihara, Y. Hanawa, T. Hamada, Predicting Effect of Cold Rolling on Fatigue Strength under Combined Loading, *Kobelco Technology Review* 30 (2011) 7-12.
- [10] T. Hanaki, Y. Hayashi, H. Akebono, M. Kato, A. Sugeta, Effect of compression Residual Stress on Fatigue Properties of Stainless Cast Steel, *Procedia Structural Integrity* 2 (2016) 3143-3149, DOI: <https://doi.org/10.1016/j.prostr.2016.06.392>.
- [11] H.K. Kim, S.M. Lee, T. Altan, Prediction of hardness distribution in cold backward extruded cups, *Journal of Materials Processing Technology* 59/15 (1996) 113-121, DOI: [https://doi.org/10.1016/0924-0136\(96\)02292-3](https://doi.org/10.1016/0924-0136(96)02292-3).
- [12] H. Tumer, F.O. Sonmez, Optimum shape design of die and preform for improved hardness distribution in cold forged parts, *Journal of Materials Processing Technology* 209 (2009) 1538-1549, DOI: <https://doi.org/10.1016/j.jmatprotec.2008.04.017>.
- [13] A. Demir, F.O. Sonmez, Prediction of Brinell Hardness Distribution in Cold Formed Parts, *Transactions of the ASME* 126 (2004) 398-405, DOI: <https://doi.org/10.1115/1.1789960>.
- [14] Exhaust valve spindle inspection and acceptance criteria, *Man Diesel & Turbo*, 2016.